

Deep-Bed Filtration Under Multiple Particle-Capture Mechanisms

R.G. Guedes, SPE, North Fluminense State University, LENE; F. Al-Abduwani, SPE, Delft University of Technology; P. Bedrikovetsky,* SPE, North Fluminense State University, LENE; P.K. Currie, SPE, Delft University of Technology

Summary

Severe injectivity decline during seawater injection and produced-water reinjection is a serious problem in offshore waterflood projects. The permeability impairment occurs because of the capture of particles from injected water by the rock, both internally in the pores and externally in a filter cake. The reliable modeling-based prediction of injectivity decline is important for injected-water-treatment design and management (injection of seawater or produced water, water filtering, etc.).

The classical deep-bed filtration model includes a single overall description of particle capture. During laboratory or field data interpretation using this model, it is usually assumed that several simultaneously occurring capture mechanisms are represented in the model by a single overall mechanism. The filtration coefficient, obtained by fitting the model to the laboratory or field data, represents the total kinetics of the particle capture. The purpose of this study is to justify this approach of using an aggregated single filtration coefficient.

A multiple-retention deep-bed filtration model needs to describe several simultaneous capture mechanisms. The kinetics of the different capture mechanisms can differ from one another by several orders of magnitude. This greatly affects the particle propagation in natural reservoirs and the resulting formation damage. In this study, a model for deep-bed filtration taking into account multiple particle-retention mechanisms is discussed. It is proven that the multicapture model can be reduced to a single-capture-mechanism deep-bed filtration model. The method for determination of the capture kinetics for all individual capture processes from the breakthrough curve is discussed. As an example, the complete characterization of filtration with monolayer and multilayer deposition of iron oxide colloids is performed using particle-breakthrough curves from coreflooding.

Introduction

Deep-bed filtration of particle suspensions in porous media occurs during seawater/produced-water injection in oil reservoirs, drilling-fluid invasion into reservoir productive zones, sand filtration in gravel packs, fines migration in oil fields, industrial filtering, etc. (Barkman and Davidson 1972; Schechter 1992). The basic features of the process are particle capture by the porous medium and the consequent permeability reduction (Nabzar et al. 1997; Roque et al. 1995). Deep-bed filtration also occurs in several environmental processes, such as produced-water disposal in aquifers; virus, bacteria, and other contaminant propagation in ground water reservoirs; etc. (Khilar and Fogler 1998; Elimelech et al. 1995). Design and planning of the mentioned technological and environmental processes should be based on reliable mathematical modeling.

Of course, deep-bed filtration is not the only mechanism that is important during such processes. Filter-cake formation on the surface of the injection well also plays a very important role. For low pore throat to particle size ratios, the formation of the filter

cake may be the dominant cause of loss of injectivity. Nevertheless, understanding of deep-bed filtration mechanisms is in many cases essential for understanding loss of injectivity in a reservoir.

The traditional mathematical model for deep-bed filtration taking into account advective particle transport and the kinetics of particle retention have been based on the filtration equation proposed by Iwasaki (1937; Herzig et al. 1970). The model accounts for a single capture mechanism. A number of predictive models have been presented in the literature (Pand and Sharma 1994; Wennberg and Sharma 1997; Bedrikovetsky et al. 2002; Al-Abduwani et al. 2004). The equations allow for various analytical solutions, which have been used for the treatment of laboratory data (Eylander 1988; van Oort et al. 1993; Bedrikovetsky et al. 2001, 2003; Al-Abduwani et al. 2005). Herzig et al. (1970) present a detailed description of such early work in a review paper.

The model has been successfully applied in several injectivity-prediction studies (Sharma et al. 2000; Bedrikovetsky et al. 2005). Nevertheless, particles are captured in the reservoir because of different physical forces and mechanisms: size exclusion, surface sorption, electrical forces, sedimentation, diffusion, etc. (Nabzar et al. 1997; Roque et al. 1995; Elimelech et al. 1995). Therefore, questions arise: What are the dominant capture processes? How does one account for several capture mechanisms (Chauveteau et al. 1998; Veerapen et al. 2001)? The filtration coefficient in the traditional single capture model is a summation of the filtration effects for all capture mechanisms; it is an effective phenomenological parameter in a multicapture environment. The purpose of this study is to justify the approach of using an aggregated single filtration coefficient.

The role of multiple simultaneous particle-capture processes has long been recognized. Network models account for several mechanisms of particle capture (Payatakes et al. 1973, 1974; Imdakm and Sahimi 1991; Sahimi and Imdakm 1991). Numerous capture processes, including internal filter-cake development, have been implemented in the microscale computer model (Nabzar et al. 1997; Roque et al. 1995; Chauveteau et al. 1998; Veerapen et al. 2001). The model allows calculation of the retention rate for all the implemented mechanisms.

Pore-scale models distinguish between size exclusion on pore throats and capture inside the pore (Sahimi and Imdakm 1991; Rege and Fogler 1987, 1988; Siqueira et al. 2003). The phenomenological capture probability is a parameter that aggregates electrical attraction, sorption, and segregation in a pore body.

In this study, we show that a multiple capture model can be reduced to that with a single capture filtration coefficient. This overall filtration coefficient can be expressed in terms of the filtration coefficients for all capture mechanisms. It allows for the determination of all individual filtration coefficients from experimental breakthrough curves as obtained from laboratory coreflooding. These relatively simple laboratory tests can be performed on cores taken from the formation into which injection is taking place, using representative samples of injection water. This gives a direct prediction of injectivity behavior in the field.

The structure of the paper is as follows. First, we introduce the classical single-capture model for deep-bed filtration along with the analytical solution with a constant filtration coefficient. Then follow equations for multicapture suspension transport and their reduction to a single capture model. Several examples of aggregation of multiple particle capture to a single capture process are presented. Then, the analytical model for a single capture

* Currently at University of Adelaide, Australia.

filtration is presented along with the solution of inverse problem for filtration function determination from the breakthrough curve. Finally, an optimization algorithm for determination of individual filtration coefficients from the breakthrough curve is discussed and applied for treatment of laboratory data on transport of iron oxide colloids in packed quartz sand media with monolayer and multilayer deposition.

Deep-Bed Filtration With a Single Particle-Capture Mechanism

Let us consider the classical deep-bed filtration model (Iwasaki 1937; Herzog et al. 1970). Strictly speaking, it accounts for a single capture mechanism. Nevertheless, it is used for injectivity prediction in real field cases (Sharma et al. 2000; Bedrikovetsky et al. 2005), assuming that the single capture rate is an aggregate for all capture mechanisms (Fig. 1). In a routine laboratory coreflood, designed for complete characterization of single-capture deep-bed filtration, outlet suspended concentration and pressure drop over the core are measured during the test. These parameters are common for all capture mechanisms, so the single capture modeling approach is self-consistent if the coreflood is performed strictly under the natural reservoir conditions.

The deep-bed filtration model consists of equations for particle mass balance, kinetics of the particle capture, and the modified Darcy's law that accounts for permeability reduction caused by particle capture (Iwasaki 1937; Herzog et al. 1970):

$$\begin{cases} \frac{\partial C}{\partial T} + \frac{\partial C}{\partial X} = -\frac{\partial S}{\partial T} \\ \frac{\partial S}{\partial T} = \Lambda(S)C \\ U = -\frac{k_0 \kappa(S)}{\mu L} \frac{\partial p}{\partial X} \end{cases}, \dots \dots \dots (1)$$

where dimensionless length, time, and concentrations are given by the following formulas:

$$\begin{aligned} X &= \frac{x}{L}; T = \frac{1}{L\phi} \int_0^t U(t) dt; \\ C &= \frac{c}{c^0}; S = \frac{\sigma}{\phi c^0}; \Lambda = \lambda L. \end{aligned} \dots \dots \dots (2)$$

In Eqs. 1 and 2, C is the dimensionless suspended particle concentration (Fig. 3), S is the dimensionless deposited particle concentration (number of captured particles per unit of the rock volume), ϕ is the porosity, L is the core length. The dimensionless filtration coefficient $\Lambda(S)$ expresses the particle capture intensity. The formation damage function $\Lambda(S)$ shows how permeability decreases because of particle retention.

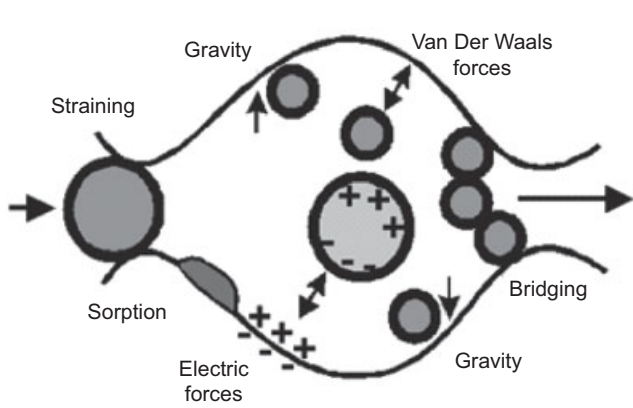


Fig. 1—Schematic of multiple capture mechanisms in natural rock during water injection.

The velocity U is independent of the linear coordinate X because of the aqueous suspension incompressibility. In addition, we have assumed that the porosity ϕ is constant and is unaffected by the deposition. This may not be the case when significant deposition takes place.

The first two equations in Eq. 1 represent the kinematics of particle transport and capture; the third equation is a dynamical model that predicts pressure gradient increase caused by permeability decline with particle deposition. The third equation decouples from the first and second equations so the system of two kinematic equations can be solved independently.

The initial and boundary conditions for particulate suspension injection into a porous medium filled by a particle-free fluid are

$$T = 0 : C = 0, S = 0; X = 0 : C = 1. \dots \dots \dots (3)$$

In the case of constant filtration coefficient, the solution of the initial-boundary value problem Eqs. 1 and 3 for $T > X$ is (Herzog et al. 1970; Pang and Sharma 1997):

$$\begin{aligned} C(X, T) &= \exp(-\Lambda X) \\ S(X, T) &= \Lambda(T - X) \exp(-\Lambda X). \end{aligned} \dots \dots \dots (4)$$

Ahead of the concentration front $T < X$, both concentrations are zero.

The suspended concentration distribution reaches the steady state given by Eq. 4 for the overall core at the moment $T = 1$. Therefore, for the case of constant filtration coefficient, the outlet concentration is equal to zero before the particle breakthrough $T < 1$, and is constant afterward. After $T = 1$, the deposition rate becomes constant. The deposit accumulates, and the deposited concentration grows proportionally to time, given by Eq. 4.

The explicit formula for suspended concentration allows calculation of the constant filtration coefficient from the constant outlet concentration (Pang and Sharma 1997; Wennberg and Sharma 1997). For the more general case when λ is not a constant, $\Lambda = \Lambda(S)$ and the breakthrough curve $C(1, T)$ determines the filtration coefficient. The solution of the inverse problem is unique and stable (Bedrikovetsky et al. 2002; Alvarez 2004).

Eq. 4 allows for the following physical interpretation of the filtration coefficient. The average particle penetration depth is equal to $1/\lambda$.

$$\int_0^\infty x c(x, t) dx / \int_0^\infty c(x, t) dx = \frac{1}{\lambda} \dots \dots \dots (5)$$

It is worth mentioning that particles move with the carrier water velocity according to the continuity equation. The analytical solution for 1D deep-bed filtration includes a suspended concentration shock that moves with the carrier water velocity along the trajectory $X = T$.

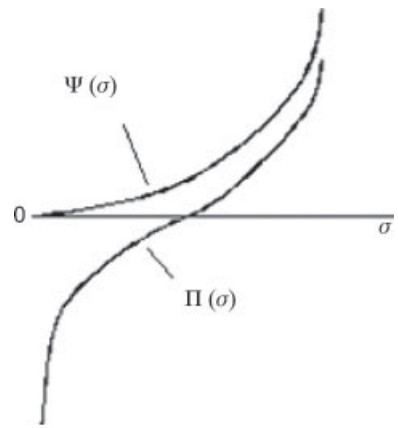


Fig. 2—Shape of functions in the analytical model.

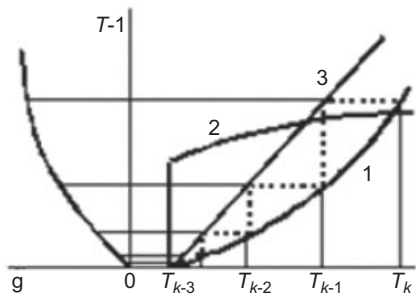


Fig. 3—Iterative procedure for solving the first inverse problem.

Mathematical Model for Transport and Multiple Capture of Particles

Consider injection of a particle suspension into a porous reservoir. The retained particle concentrations deposited by all capture mechanisms $\sigma_1, \sigma_2 \dots \sigma_n$ are introduced (Fig. 1). It is assumed that each mechanism capture rate is proportional to the particle flux cU , and that the corresponding filtration coefficients $\lambda_1, \lambda_2 \dots \lambda_n$ are dependent on all $\sigma_1, \sigma_2 \dots \sigma_n$.

We note that the assumption that each capture rate is proportional to cU is essential for the analysis that follows. This may not be a valid assumption, especially if shear mechanisms within the pore play a significant role. However, the experimental evidence shows that this proportionality assumption is generally reasonable and is, at least approximately, true.

The system of governing equations consists of the mass balance for retained and suspended particles and of capture kinetics for each mechanism:

$$\frac{\partial}{\partial t} \left(\phi c + \sum_{i=1}^n \sigma_i \right) + U \frac{\partial c}{\partial x} = 0 \dots \dots \dots (6)$$

and

$$\frac{\partial \sigma_i}{\partial t} = \lambda_i (\sigma_1, \dots \sigma_n) c U, i = 1, 2 \dots n. \dots \dots \dots (7)$$

As for the case of the single-capture model, we assume that the porosity ϕ is constant and unaffected by deposition. Introduction of the dimensionless coordinates and parameters defined in Eq. 2, along with

$$S_i = \frac{\sigma_i}{\phi c_0}; \Lambda_i = \lambda_i L \dots \dots \dots (8)$$

transforms Eqs. 6 and 7 to

$$\frac{\partial}{\partial T} \left(C + \sum_{i=1}^n S_i \right) + \frac{\partial C}{\partial X} = 0 \dots \dots \dots (9)$$

and

$$\frac{\partial S_i}{\partial T} = \Lambda_i (S_1, \dots S_n) C, i = 1, 2 \dots n. \dots \dots \dots (10)$$

Initial conditions correspond to particle absence in the reservoir before the injection.

$$T = 0 : C = S_i = 0. \dots \dots \dots (11)$$

Boundary conditions correspond to a given suspended concentration in the injected fluid.

$$X = 0 : C = 1. \dots \dots \dots (12)$$

The injected water front will propagate into the porous medium with unit dimensionless speed. Suspension and retained concentrations are zero ahead of the injected-water front (Appendix A), like

in a single capture system. Retained concentrations are continuous across the front and, therefore, are zero on the concentration front. From the characteristic form of the system (Eqs. 9 and 10) follows the exponential decrease of suspended concentration on the front.

$$C(T, T) = \exp \left(- \sum_{i=1}^n \Lambda_i (0, 0 \dots 0) T \right) \dots \dots \dots (13)$$

Examples of Models With Multiple Capture Mechanisms

To illustrate the variety of models that fall under the multicapture model formulated in the previous section, we consider a few examples. First, let us discuss deep-bed filtration of hematite particles with monolayer and polylayer adsorption. The process has been analyzed and modeled numerically by Kuhnen et al. (2000).

The hematite particles are exposed to two types of capture in porous quartz sand: monolayer adsorption with blocking of free grain surface driven by particle/surface interaction, and multilayer adsorption caused by particle/particle interaction. The two capture mechanisms have different kinetic rates and different characteristic times.

The blocking kinetics are described by the fraction θ of the bare surface covered with colloidal particles. The mathematical model consists of mass balance for suspended and retained particles (Eq. 1), the total kinetics equation:

$$\frac{\partial S}{\partial T} = \zeta [B(\theta) + \epsilon \theta] C \dots \dots \dots (14)$$

and the blocking monolayer kinetics

$$\frac{\partial \theta}{\partial T} = \gamma B(\theta) C. \dots \dots \dots (15)$$

Here, ζ and γ are dimensionless constants defined in Appendix D, and $B(\theta)$ is a blocking function. We discuss the case of Langmuir adsorption that is typical for medium concentration suspension, where the retention alters the grain surface available for adsorption and the suspended particles do not interact with each other.

$$B(\theta) = 1 - \beta \theta. \dots \dots \dots (16)$$

The system of Eqs. 1, 14, and 15 can be translated into the form of Eqs. 9 and 10. However, this adds unnecessary intermediate calculations. As shown in Appendix D, straightforward calculation of $S = S(\theta)$ can be performed directly from Eqs. 14 and 15.

Another example of two-capture deep-bed filtration system was studied by Rege and Fogler (1987, 1988) and Siqueira et al. (2003). Pore space is presented by a cubic lattice with pores placed in lattice vortices. Sides represent the capillary with pore throat radii. Several particle retention processes inside the pore (Fig. 1) are represented by one aggregated capture mechanism by giving the probability for a particle to be captured inside the pore body. Size exclusion takes place at pore exits—a particle larger than the pore throat does not pass into a capillary.

Size exclusion in a system with a size distribution of both particles and pores (Sharma and Yortsos 1987) can be also described by a multicapture system (Eqs. 9 and 10). The system with incomplete pore plugging (Shapiro et al. in press) allows for an analytical solution in case of single particle size injection and a medium with two pore sizes. The particle is smaller than the large pore and is larger than the small pore. Each capture decreases the pore size; the small pore radius after n sequential retentions is considered to be zero. Therefore, “new” pores appear because of the partial plugging with $n-1$ different radii. The degree of freedom of the system is n , and the equations have the type of Eqs. 9 and 10.

Reduction of the Multicapture System to That of a Single Capture Mechanism

We now show that the system for deep-bed filtration with n simultaneous particle-capture mechanisms can be reduced to the single-capture system: All simultaneous capture processes can be

aggregated into a single capture process with a filtration coefficient that equals the sum of the filtration coefficients of all simultaneous capture processes. The total filtration coefficient can be expressed as a function of the total retained concentration.

The n -capture system (Eqs. 9 and 10) has n degrees of freedom (Landau and Lifshitz 1980; Bedrikovetsky 1993). Let us sum Eq. 10 from 1 to n ; the total deposition rate is proportional to the total filtration coefficient (the sum of all the individual filtration coefficients) that is a function of all individual retention concentrations (i.e., the system still has n degrees of freedom). Derivations in Appendix B show that the total filtration coefficient can be expressed in terms of the total deposition concentration (i.e., the degrees of freedom for the system of Eq. 10 can be reduced to 1).

Let us denote by

$$S_i = f_i(S) \dots\dots\dots (17)$$

the solution of the Cauchy problem

$$S = 0 : S_i(S) = 0 \dots\dots\dots (18)$$

for the system of ordinary differential equations

$$\frac{dS_i}{dS} = \frac{\Lambda_i(S_1, \dots, S_n)}{\sum_{i=1}^n \Lambda_i(S_1, \dots, S_n)}, i = 1, 2 \dots n \dots\dots\dots (19)$$

Eq. 17 allows the expression of the total filtration coefficient as a function of the overall deposition concentration.

$$\Lambda(S) = \sum_{i=1}^n \Lambda_i(S_i(f_i(S)), \dots, S_n(f_n(S))) \dots\dots\dots (20)$$

As shown in Appendix B, the system of multicapture filtration becomes the same as Eq. 1. Aggregation of all individual filtration coefficients (Eq. 7) into a single filtration coefficient (Eq. 20) allows reduction of the multicapture $(n + 1) \times (n + 1)$ system (Eqs. 6 and 7) to the 2×2 system (Eq. 1).

Examples of the Aggregation of Multicapture Models Into a Single Filtration Coefficient

Let us discuss some examples of aggregation of multicapture deep-bed filtration models into the form with a single capture coefficient. First, we consider n simultaneous retention processes during flow of a low-concentration suspension. For low-concentrated suspensions, the total retained concentration is also low. The deposition does not alter the pore space geometry and surface area of the rock, and the filtration coefficient can be considered to be constant. For medium-concentration suspensions, the filtration coefficient can be considered constant for small times. If all filtration coefficients in Eq. 7 are constant, the sum of Eq. 7 from $i = 1$ to $i = n$ leads to the conclusion that the total filtration coefficient λ is equal to the sum of all individual filtration coefficients λ_i and is also constant.

The second example, analyzed in Appendix C, has two simultaneous capture mechanisms, where the first filtration coefficient λ_1 is a linear function of retained concentration, and the second filtration coefficient λ_2 is constant. This model is relevant for medium-concentration suspensions where particle retention alters the rock surface available for capture but suspended particles do not interact. One can formulate the kinetic equation as

$$\frac{\partial \sigma}{\partial t} = \lambda_0 h c U, \dots\dots\dots (21)$$

where h is the concentration of vacancies available for particle capture. It is assumed that a vacancy is filled by m retained particles, so the vacancy concentration can be expressed in terms of the retained concentration $h(x,t) = h(x, 0) - m^{-1} \sigma(x,t)$. Substituting into Eq. 21, we obtain

$$\frac{\partial \sigma}{\partial t} = \lambda_0 (h_0 - m^{-1} \sigma) c U, \dots\dots\dots (22)$$

assuming the initial vacancy concentration $h(x,0) = h_0$ is uniform. From Eq. 22 follows that the filtration coefficient is a linear function of retained concentration:

$$\lambda_1(\sigma) = \lambda_0 (h_0 - m^{-1} \sigma) \dots\dots\dots (23)$$

Such a linearly dependent filtration coefficient is considered in several studies where medium-concentration suspensions are used (Kuhnen et al. 2000; Soo et al. 1986). Appendix C shows that the total filtration coefficient is

$$\lambda(\sigma) = \lambda_0 (h_0 - m^{-1} \sigma) + \lambda_2, \dots\dots\dots (24)$$

where $\sigma_1(\sigma)$ is the inverse to the function in Eq. C-3.

The third example considers a quadratic filtration function for the first capture mechanism; the second filtration coefficient is constant.

$$\lambda_1 = a(S_1 + b)^2, \lambda_2 = d \dots\dots\dots (25)$$

The quadratic filtration function describes either increase or decrease of the deposition rate during retention (Roque et al. 1995; Veerapen 2001). The quadratic filtration function describes either increase or decrease of the deposition rate during retention. A decreasing rate can describe blocking behavior because it reduces to zero, remaining zero for higher retention concentration. It also describes a non-monotonic filtration coefficient variation during the increase of retained concentration. All the previously mentioned cases can be obtained by choosing the respective signs for coefficients a , b , and d of the quadratic polynomial (Eq. 25). Integration of the system of Eqs. 9 and 10 for the case of Eq. 25 is presented in Appendix C. The total filtration function is found to be

$$\lambda(S) = d + \frac{a}{4} \left(S - \frac{d}{ab} + b \pm \sqrt{\left(S - \frac{d}{ab} - b \right)^2 + 4Sb} \right)^2 \dots\dots\dots (26)$$

For deep-bed filtration of hematite particles in sand packs with monolayer and polylayer adsorption, the derivation of the aggregation is presented in Appendix D. The overall filtration coefficient is given by Eqs. D-9 and D-10.

Analytical Model for a Single-Capture-Mechanism Deep-Bed Filtration

The initial and boundary conditions (Eq. 3) for Eq. 1 correspond to the problem of particle suspension injection into a particle-free porous reservoir or core. This problem has an exact analytical solution (Herzig et al. 1970; Bedrikovetsky et al. 2002). Introduction of the potential

$$\Pi(S) = \int_0^S \frac{d\sigma}{\Lambda(\sigma)} \dots\dots\dots (27)$$

allows transforming the second part of Eq. 1 to the form

$$\frac{\partial \Pi(S)}{\partial T} = C \dots\dots\dots (28)$$

Substitution of Eq. 28 into the first part of Eq. 1 and integration in T from zero to T , allowing for the initial conditions (Eq. 3), results in the following first-order quasilinear partial differential equation

$$\frac{\partial S}{\partial T} + \frac{\partial S}{\partial X} = -\Lambda(S)S \dots\dots\dots (29)$$

Fixing $C = 1$ in the second part of Eq. 1 for the inlet $X = 0$ provides the boundary condition for Eq. 29.

$$X = 0: \Pi(S) = T. \dots\dots\dots (30)$$

The solution of the problem (Eqs. 1 and 2) is obtained by the method of characteristics

$$\int_{\Pi^{-1}(T-X)}^{S(X,T)} \frac{dS}{\Lambda(S)S} = X \dots\dots\dots (31)$$

Here, $\Pi^{-1}(T)$ is an inverse function to Eq. 27. It expresses retained concentration $S(0,T)$ at the inlet from Eq. 30. The solution $S(X,T)$ can be expressed via the primitive of the integral in Eq. 31.

$$\Psi(S(X,T)) - \Psi(\Pi^{-1}(T-X)) = X$$

$$\Psi = \int \frac{dS}{\Lambda(S)S} \dots\dots\dots (32)$$

Typical plots of functions Π and Ψ are shown in **Fig. 2**. After finding the retained concentration $S(X,T)$ from Eqs. 31 and 32, one obtains the suspended concentration $C(X,T)$ directly from Eq. 28.

Analytical Model for a Multiple-Capture Deep-Bed Filtration

The analytical solution for the multiple capture problem (Eqs. 9 and 10) directly follows from the single-capture solution (Eqs. 31 and 32) and from the aggregation procedure (Eqs. 17 through 20). From this procedure follows that the suspended concentration $C(X,T)$ and the total retained concentration $S(X,T)$ from multiple capture system (Eqs. 9 and 10) already satisfy the single-capture system (Eq. 1) with initial and boundary conditions (Eq. 3) and with the aggregated total filtration coefficient (Eq. 20). Eq. 17 provides the retained concentration distribution for each component. Eqs. 17, 31, and 32 form an analytical solution for the multiple-capture deep-bed filtration of particulate suspensions.

Characterization of Single-Capture Deep-Bed Filtration System From Laboratory Data: Inverse Problems

The single-capture system (Eq. 1) contains an empirical filtration function $\Lambda(S)$. We now show how to obtain it from the effluent concentration history $C(1,T)$, the so-called breakthrough curve (Bedrikovetsky et al. 2002; Alvarez 2004), in a laboratory test in which a constant concentration suspension is injected into a core with measurement of exit suspension concentration and pressure drop over the core.

Let us integrate Eq. 28 from 1 to T for $X = 1$:

$$\Pi(\sigma(1, T-1)) = M(T-1),$$

$$\sigma(1, T-1) = g(M(T-1)), \dots\dots\dots (33)$$

where M is the accumulated mass of produced particles

$$M(T-1) = \int_0^{T-1} C(1, \ell+1) d\ell \dots\dots\dots (34)$$

and $g(T) = \Pi^{-1}(T)$ is the inverse function of Eq. 27.

The iterative procedure for solving the functional equation (Eq. 33) is shown graphically in Fig. 3. It is very easy to implement numerically. Curves 1, 2, and 3 in this figure correspond to the functions $M(T)$, $C(1,T)$, and $T-1$, respectively. The value of $g'(T)$ follows from differentiating Eq. 30 near $T = X = 0$.

$$g'(0) = \lambda(0) \dots\dots\dots (35)$$

The filtration coefficient $\lambda(\sigma)$ can be found from the function $\sigma = g(\Psi)$ using Eq. 27. Once $\lambda(\sigma)$ has been determined, the retained concentration $S(X,T)$ can be found by solving Eqs. 1 and 3.

For a multiple-capture-mechanism system, the formation damage κ will be a function of all retained concentrations, because the same retained concentrations for particles captured by different mechanisms (e.g., size exclusion and sorption) will cause completely different permeability damage.

$$\kappa = \kappa(S_1, S_2 \dots S_n) \dots\dots\dots (36)$$

Substitution of the Eq. 17 into Eq. 36 realizes the aggregation of different retained components into a single-variable formation damage function $\kappa(S)$:

$$\kappa(S) = \kappa(f_1(S), f_2(S) \dots f_n(S)) \dots\dots\dots (37)$$

If we measure pressure drop $\Delta p(T)$ on the core during suspension injection, then integrating Darcy's law (the third part of Eq. 1) over the length of the core we get

$$\int_0^1 \frac{dX}{\kappa(S(X,T))} = \Delta p(T) \dots\dots\dots (38)$$

This is an integral equation that determines the positive function $\kappa(\sigma)$. If a good guess of $\kappa(\sigma)$ is available, Tichonov's regularization can be used as iterative procedure to solve Eq. 36. Optimization methods can be used to find the initial guess. The details of this procedure can be found in the thesis of Alvarez (2004).

Therefore, from the breakthrough curve, one determines an overall filtration function. Once the filtration function is determined, the formation-damage function is calculated from the pressure drop over the core. Splitting overall filtration function into filtration functions for each capture mechanism $\lambda_i(S_1, S_2, \dots S_n)$ is a separate problem, discussed later.

Several environmental processes require the forecast of suspension propagation in reservoirs and are not concerned with the retained concentration. In this case, the laboratory coreflood tests must be performed under reservoir conditions (i.e., maintenance of the same reservoir temperature and pressure, water salinity, and mineral rock composition as that in a natural reservoir) to provide the same capture rate for all the retention mechanisms. The functions $\lambda_i(S_1, S_2, \dots S_n)$ are then the same in the laboratory as in the reservoir. An overall filtration function must be determined. As follows from the aggregation procedure, the suspended concentration $C(X,T)$ of contaminant in the natural reservoir with multiple capture mechanisms can be described by the single-capture model (Eq. 1).

Because particle deposition during suspension propagation in natural reservoirs does not alter streamlines for 3D flows, the aggregation procedure is valid for conditions along each streamline. Therefore, the overall filtration function obtained in the laboratory can be used for 3D modeling of contaminant propagation in the natural reservoir.

Determination of Multicapture Filtration Coefficients From Breakthrough Curve

The exact solution of the inverse problem (Bedrikovetsky et al. 2004; Alvarez et al. 2006; Alvarez 2004) allows calculation of a set of points (σ_k, λ_k) , $k = 1, 2 \dots$ for filtration coefficients $\lambda_k(\sigma_k)$. For a single-capture filtration coefficient, if there is an explicit parametric formula $\lambda = \lambda_k(\sigma, b_1, b_2 \dots)$, the parameters $b_1, b_2 \dots$ can be determined by an optimization procedure, fitting the breakthrough curve to that simulated (Alvarez 2004).

In multiple-capture filtration, if explicit parametric formulas for all filtration coefficients are not available, the exact inverse solution still provides the overall filtration coefficient. But, in this case, the overall filtration coefficient cannot be split into those for all capture processes. However, if in multiple-capture filtration, explicit parametric formulas $\lambda_i(\sigma_1, \sigma_2 \dots) = \lambda_i(\sigma, b_{i1}, b_{i2} \dots)$, $i = 1, 2 \dots n$ are available, the aggregation procedure allows a single-capture optimization algorithm of the inverse problem to be used to determine the filtration coefficients for all capture mechanisms from the breakthrough curve. The solution (Eq. 17) provides expressions for the aggregated filtration coefficient $\lambda = \lambda(\sigma, b_{11}, b_{12} \dots b_{1n}, b_{21}, b_{22} \dots b_{mn})$. The full set of parameters $(b_{11}, b_{12} \dots b_{1n}, b_{21}, b_{22} \dots b_{mn})$

TABLE 1—PARAMETERS FOR PREDICTION OF BREAKTHROUGH CURVES IN FIG. 4a BY ANALYTICAL MODEL

Data	β	γ	ζ	ε
Curve 1	6.62	0.016	3.06	0
Curve 2	4.87	0.010	2.10	0
Curve 3	2.23	0.009	1.89	0
Curve 4	1.20	0.010	1.90	0.055
Curve 5	1.43	0.012	2.51	0.326
Curve 6	1.00	0.010	2.28	0.688

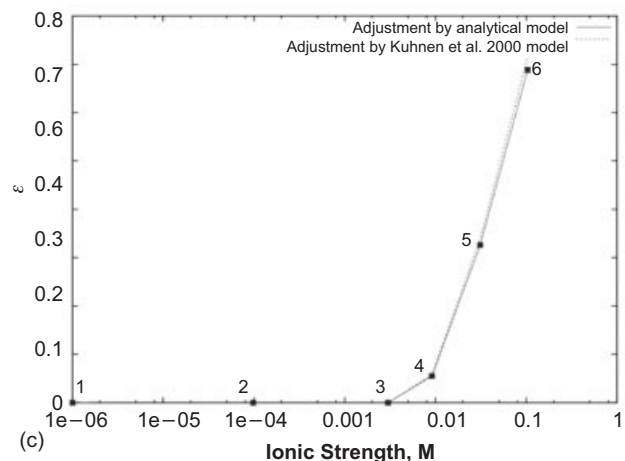
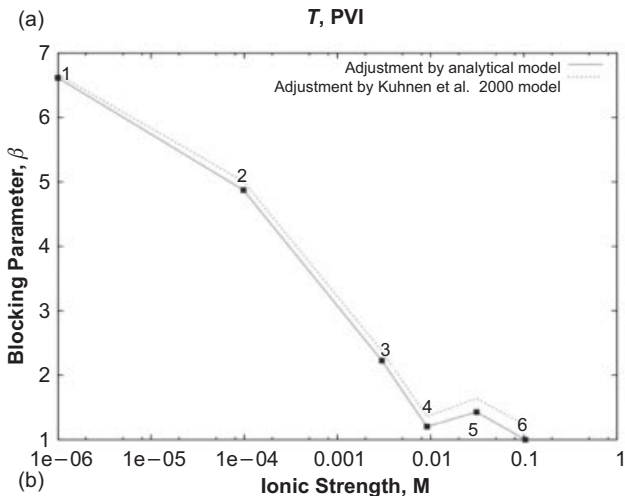
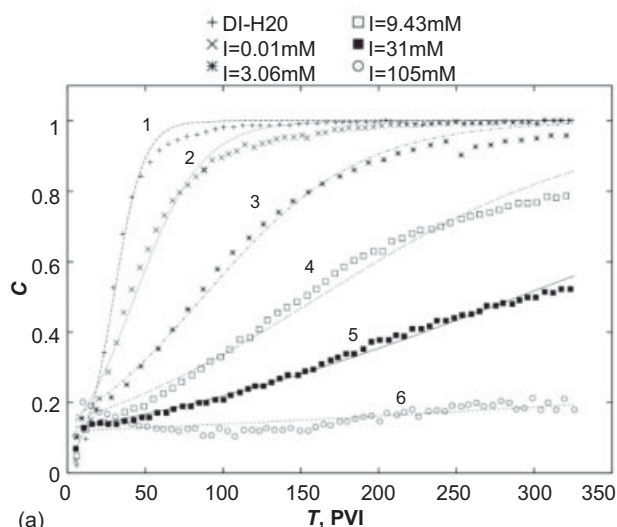


Fig. 4—Fitting of breakthrough curves by the analytical model. a) Breakthrough curves of hematite colloids through columns packed with quartz sand at different ionic strengths. Sequences of points correspond to laboratory measurements. Lines represent calculations based on estimated parameters β and ε obtained with the analytical model. b) Blocking parameter β as a function of the solution ionic strength. c) Effect of interaction ratio ε vs. ionic strength.

can be determined by optimal fitting of the breakthrough curve to that simulated using the overall filtration coefficient.

Fitting the Filtration Model of Monolayer and Poly-layer Adsorption With Laboratory Data for Hematite Particles

The analytical model for deep-bed filtration of hematite particles with monolayer and poly-layer adsorption was used to adjust the

laboratory data on hematite retention in quartz sand packs obtained by Kuhnen et al. (2000). The formulas are derived in Appendix D (see Eqs. D-9 and D-10). The outlet suspended concentration $C(1, T)$ is predicted to depend on two fitting parameters four parameters β and ε , defined in Eq. D-4. Note that we do not make the simplification $\varepsilon = 0$, discussed at the end of Appendix D and leading to Eq. D-12, but use the full expression (Eq. D-10) for the filtration coefficient.

Six experimental breakthrough curves are available, as shown in Fig. 4a, corresponding to corefloods using different salinity brines. As shown in Appendix D, the number of independent parameters for fitting is two, the blocking parameter β and the interaction ratio ε .

These two parameters were adjusted by Kuhnen et al. (2000) using a numerical model for the system (Eqs. D-1, D-2, and D-3). The Levenberg–Marquardt method (More et al. 1980) was used to estimate the two parameters by minimizing the sum-squared errors between the experimental and theoretical particle-breakthrough profiles. We use the same algorithm to estimate β and ε using the analytical model (Eqs. D-9 and D-10). The blocking parameter β obtained from fitting the six breakthrough curves with the analytical model is shown in Fig. 4b by a solid line. The dotted line presents the results obtained by Kuhnen et al. (2000). The interaction ratio ε is presented in Fig. 4c. The parameter values are given in Table 1.

One can see that the results almost coincide. Some minor discrepancy can be explained by the exclusion of hydrodynamic dispersion in our analytical model. Khunen et al. (2000) include dispersion. However, the dimensionless Péclet number for the case of hydrodynamic dispersion in porous media is equal to L/α_D , where L is a core length and α_D is the rock dispersivity (Bedrikovetsky 1993). For the sand packs used (Kuhnen et al. 2000), $\alpha_D = 7 \times 10^{-4}$ m and $L = 0.03$ m. The Péclet number is thus equal to 42.8, greatly exceeding unity, and dispersion can be ignored.

The obtained values of the parameters β and ε allow prediction of the deposition dynamics. The deposition profiles are shown in Fig. 5 for $T = 10$ and 100 pore volumes injected (pvi). Fig. 5a corresponds to parameters obtained from a low-salinity Breakthrough Curve 4 (see Fig. 4a); Fig. 5b corresponds to β and ε obtained from a high-salinity Breakthrough Curve 6 (see Fig. 4a). In both cases, the blocking efficiency is varied to study the sensitivity—the two dotted curves around every continuous fitted curve correspond to $\beta \pm 1$. Fig. 6 shows the deposition profile sensitivity with respect to the interaction ratio ε .

Availability of parametric formulas for individual capture kinetics (Eqs. D-2 and D-3) allows calculation of the parameters from the breakthrough curve and the splitting of the overall retained concentration $S(X, T)$ into individual retained concentrations $S_i(X, T)$. Figs. 7 and 8 show profiles for the surface coverage fraction θ . Figs 7a and 8a correspond to parameters obtained by fitting Breakthrough Curve 4 (in Fig.4a), and Figs 7b and 8b correspond to Breakthrough Curve 6, using the same sensitivities for β and ε as in Figs 5 and 6.

Conclusions

The results of this paper are of importance for field studies of injectivity decline. Although other mechanisms, such as filter-cake buildup also may contribute to the injectivity decline of an injection

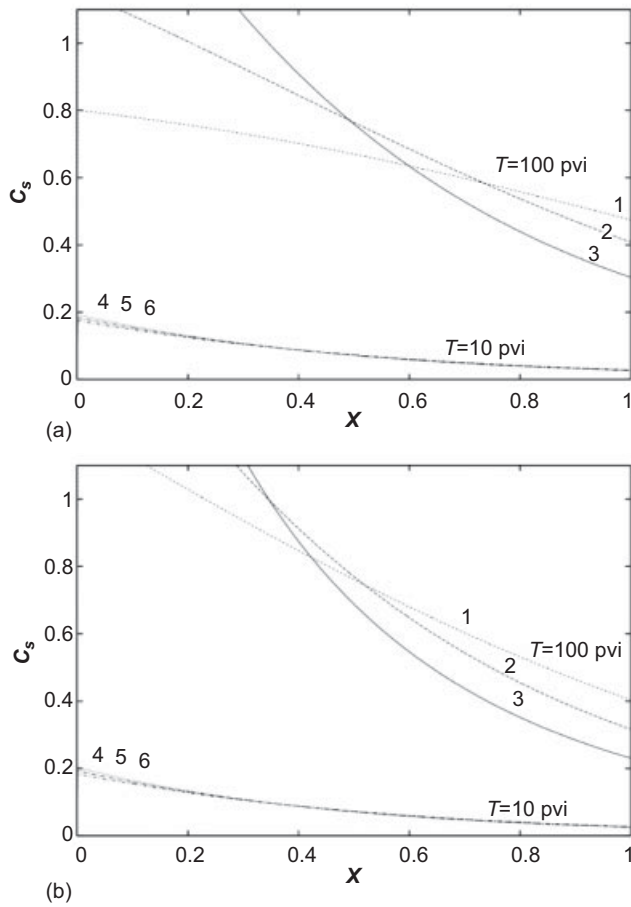


Fig. 5—Effect of blocking parameter β on deposition profiles as calculated for two times, $T = 10$ pvi and $T = 100$ pvi. (a) Deposition profiles for Breakthrough Curve 4 in Fig. 4a for $\epsilon = 0.055$: Lines 1 and 6 $\beta = 2.2$; Lines 2 and 5 $\beta = 1.20$; Lines 3 and 4 $\beta = 0.2$. (b) Deposition profiles for Breakthrough Curve 6 in Fig. 4a for $\epsilon = 0.689$: Lines 1 and 6 $\beta = 2.0$; Lines 2 and 5 $\beta = 1.00$; Lines 3 and 4 $\beta = 0$.

well, deep-bed filtration mechanisms generally also play a significant role. This study shows that the engineering approach of using an aggregated single filtration coefficient can be justified, even when multiple-capture deep-bed filtration mechanisms play a role.

A multiple-capture system of suspension transport in porous media can be reduced to an equivalent single-capture system. The retention concentration and capture rate for the aggregated single-capture system is a total of retention concentrations and capture rates for all capture mechanisms of the multiple-capture system. The filtration function for a single-capture transport is obtained from the solution of the system of ordinary differential equations; these equations include filtration functions for all capture mechanisms.

The filtration and formation damage functions of the aggregated single-capture system can be determined as a solution of the inverse problem from laboratory tests, using the breakthrough curve and the rate/pressure drop history, respectively. The laboratory tests must be performed under the same conditions as that of the reservoir (i.e., reproducing the multicapture environment).

The aggregated filtration and formation-damage functions can be used in 3D modeling of suspension transport in natural reservoirs. If particle deposition does not alter streamlines in 3D flow, the suspended concentration and pressure field for a multiple-capture system of suspension transport is the same as that for the aggregated single-capture system. In this respect, implementation of the multicapture model in a streamline simulator will be only marginally more complicated than implementation of a single-capture model because relatively few modifications of the velocity and pressure fields will be required.

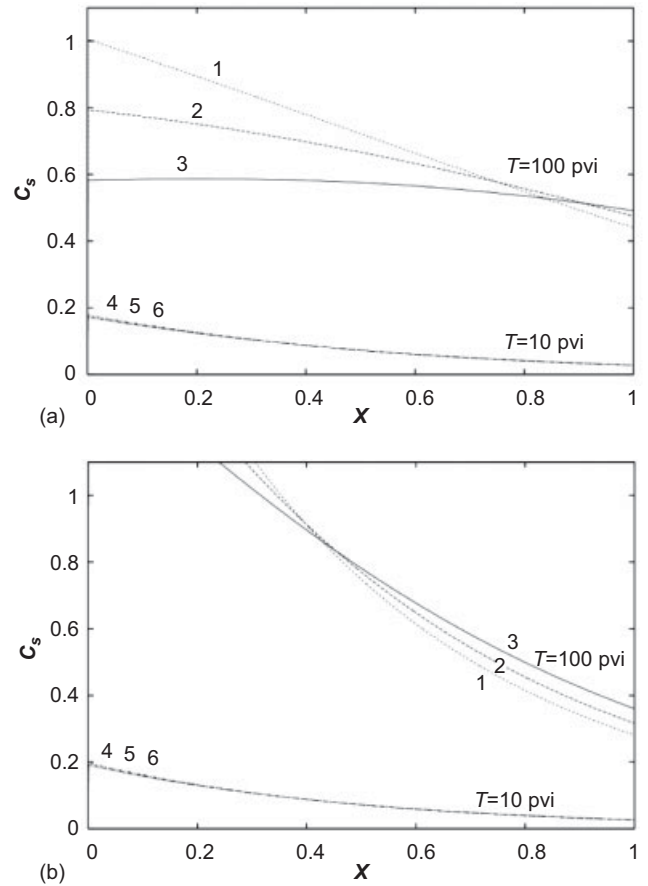


Fig. 6—Effect of interaction ratio ϵ on deposition profiles as calculated for two times, $T = 10$ pvi and $T = 100$ pvi. (a) Deposition profiles for Breakthrough Curve 4 in Fig. 4a for $\beta = 1.20$: Lines 1 and 6 $\epsilon = 0.455$, Lines 2 and 5 $\epsilon = 0.055$, Lines 3 and 4 $\epsilon = 0$. (b) Deposition profiles for Breakthrough Curve 6 in Fig. 4a for $\beta = 1.00$: Lines 1 and 6 $\epsilon = 1$, Lines 2 and 5 $\epsilon = 0.689$, Lines 3 and 4 $\epsilon = 0.289$.

Nomenclature

- a_p = grain diameter, m
- a = coefficient in the quadratic filtration function
- b = coefficient in the quadratic filtration function
- b_1, b_2, \dots = explicit parameters governing capture
- b_{j1}, b_{j2}, \dots = explicit parameters governing capture for the j th mode
- B = blocking function
- c = suspended particle concentration
- c^0 = injected suspended particle concentration
- c_z = surface concentration of deposited particles
- C = normalized suspended particle concentration
- $[C]$ = jump in C at the shock front
- d = filtration coefficient constant
- f = bare matrix area available for colloid deposition per unit pore volume
- g = inverse function of Π
- h = concentration of vacancies available for particle capture
- h_0 = initial concentration of vacancies available for particle capture
- k_0 = original permeability, m^2
- k^f = fast deposition rate
- k_{pc} = particle/matrix deposition rate
- k_{pp} = particle/particle deposition rate
- L = core length, m
- m = number of particles filling a vacancy
- M = accumulated dimensionless mass of produced particles

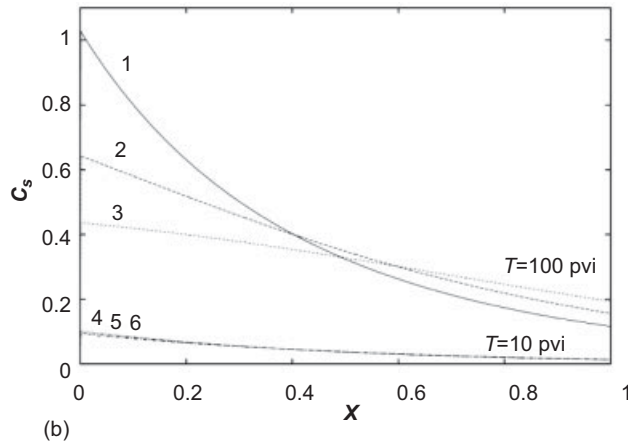
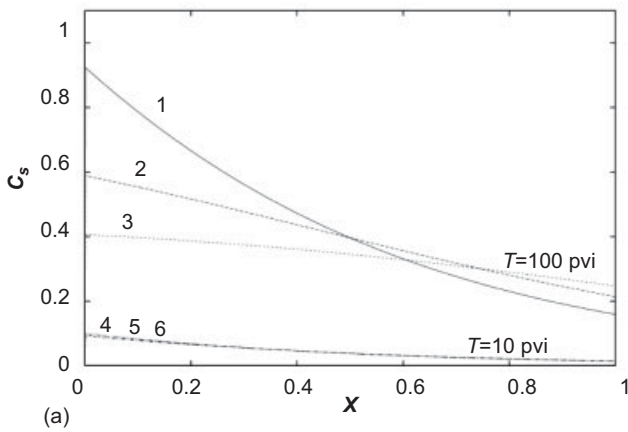


Fig. 7—Effect of blocking parameter β on surface coverage fraction profiles as calculated for two times, $T = 10$ pvi and $T = 100$ pvi. (a) Surface coverage fraction profiles for Breakthrough Curve 4 in Fig. 4a for $\varepsilon = 0.055$: Lines 1 and 6 $\beta = 2.2$, Lines 2 and 5 $\beta = 1.20$, Lines 3 and 4 $\beta = 0.2$. (b) Surface coverage fraction profiles for Breakthrough Curve 6 in Fig. 4a for $\varepsilon = 0.689$: Lines 1 and 6 $\beta = 2.0$, Lines 2 and 5 $\beta = 1.00$, Lines 3 and 4 $\beta = 0$.

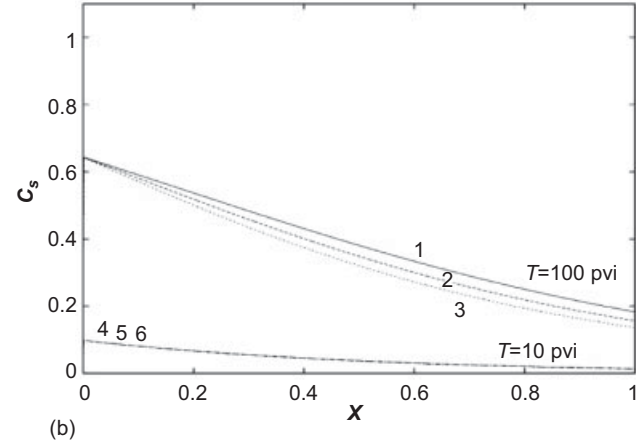
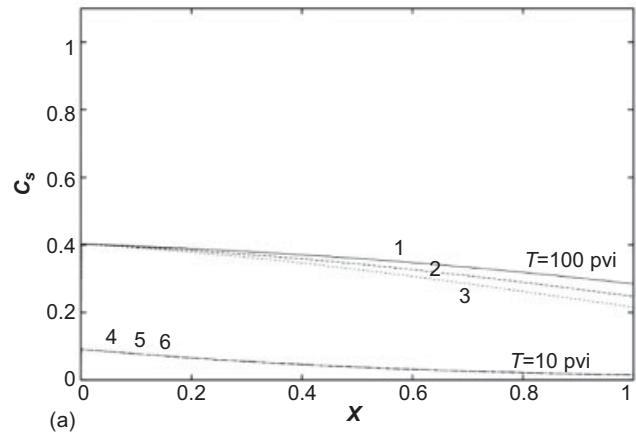


Fig. 8—Effect of interaction ratio ε on surface coverage fraction profiles as calculated for two times, $T = 10$ pvi and $T = 100$ pvi. (a) Surface coverage fraction profiles for Breakthrough Curve 4 in Fig. 4a for $\beta = 1.20$: Lines 1 and 6 $\varepsilon = 0.455$, Lines 2 and 5 $\varepsilon = 0.055$, Lines 3 and 4 $\varepsilon = 0$. (b) Surface coverage fraction profiles for Breakthrough Curve 6 in Fig. 4a for $\beta = 1.00$: Lines 1 and 6 $\varepsilon = 1$, Lines 2 and 5 $\varepsilon = 0.689$, Lines 3 and 4 $\varepsilon = 0.289$.

- n = number of capture modes
- p = pressure, Pa
- Δp = pressure drop across core, Pa
- S = normalized deposited particle concentration
- S_j = normalized deposited particle concentration for j th capture mode
- $[S_j]$ = jump in S_j at the shock front
- T = normalized time
- t = time, s
- U = total flow velocity, m/s
- v_p = average interstitial velocity of particles, m/s
- x = distance along core, m
- x_f = position of shock front, m
- α_D = rock dispersivity, m
- α_{pc} = collision efficiency for particle/matrix deposition
- α_{pp} = collision efficiency for particle/particle deposition
- β = Langmuir coefficient in linear blocking function
- γ = nondimensional parameter defined in Eq. D-4
- ε = nondimensional parameter defined in Eq. D-4
- ς = nondimensional parameter defined in Eq. D-4
- θ = fraction of bare surface covered with deposited particles
- κ = permeability reduction function
- λ = filtration coefficient, m^{-1}
- λ_j = filtration coefficient for j th capture mode, m^{-1}
- Λ = dimensional filtration coefficient
- Λ_j = dimensional filtration coefficient for j th capture mode
- μ = viscosity of the fluid, Pa·s

- Π = potential function for the inverse filtration coefficient
- σ = deposited-particle concentration
- σ_j = deposited-particle concentration for j th capture mode
- ϕ = porosity
- Ψ = primitive of integral defined in Eq. 31

Acknowledgments

This work grew out of the permanent collaboration with Petrobras colleagues Alexandre Siqueira, Antonio Luiz, and Claudio A. Furtado (Petrobras, National Brazilian Oil Company).

Collaboration with Yannis Yortsos (South California University, USA), Oleg Dinariev (Institute of Earth Physics, Russian Academy of Sciences), Dan Marchesin (Institute of Pure and Applied Mathematics, Brazil), Alexander Shapiro (Technical University of Denmark) and Adriano Santos (North Fluminense State University) is highly acknowledged.

Special thanks are due to Themis Carageorgos (North Fluminense State University) for support and encouragement.

References

- Al-Abduwani, F.A.H., de Zwart, B.-R., Farajzadeh, R., van den Broek, W.M.G.T. and Currie, P.K. 2004. Utilizing Static Filtration Experiments To Test Existing Filtration Theories for Conformance. Prepared for presentation at the 2nd NEL Produced Water Workshop, Aberdeen, 21– 22nd April.
- Al-Abduwani, F.A.H., Hime, G., Alvarez, A., and Farajzadah, R. 2005. New Experimental and Modeling Approach for the Quantification of Internal Filtration. Paper SPE 94634 presented at the SPE European

Formation Damage Conference, Sheveningen, The Netherlands, 25–27 May. DOI: 10.2118/94634-MS.

Alvarez, A.C. 2004. Inverse problems for deep bed filtration in porous media. in Department of Fluid Dynamics. PhD thesis, Instituto Nacional de Matemática Pura e Aplicada (IMPA), Rio de Janeiro, Brazil, 149 (2 August 2005).

Alvarez, A.C., Bedrikovetsky, P.G., Hime, G., Marchesin, A.O., Marchesin, D., and Rodríguez, J.R. 2006. A fast inverse solver for the filtration function for flow of water with particles in porous media. *Inverse Problems* **22**: 69–88. DOI: 10.1088/0266-5611/22/1/005.

Barkman, J.H. and Davidson, D.H. 1972. Measuring Water Quality and Predicting Well Impairment. *J. Pet Tech* **24** (7): 865–873; *Trans.*, AIME, **253**. SPE-3543-PA. DOI: 10.2118/3543-PA.

Bedrikovetsky, P., Fonseca, D.R., da Silva, M.J., da Silva, M.F., Siqueira, A.G., de Souza, A.L. S., and Furtado, C. 2005. Well-History-Based Prediction of Injectivity Decline (Accounting for Oil-Water Mobility Variation During Waterflooding). Paper SPE 93885 presented at the SPE Latin American and Caribbean Petroleum Engineering Conference, Rio de Janeiro, 25–27 June. DOI: 10.2118/93885-MS.

Bedrikovetsky, P., Marchesin, D., Hime, G., Alvarez, A.L., Marchesin, A.O., Siqueira, A.G., Souza, A.L.S., Shecaira, F.S., and Rodrigues, J.R. 2002. Porous media deposition damage from injection of water with particles. *Proc.*, 8th European Conference on the Mathematics of Oil Recovery, Freiberg, Germany, 3–6 September, E18.

Bedrikovetsky, P., Marchesin, D., Shecaira, F., Souza, A.L., Milanez, P.V. and Rezende, E. 2001. Characterization of deep bed filtration system from laboratory pressure drop measurements. *Journal of Petroleum Science and Engineering* **32** (2–4): 167–177. DOI: 10.1016/S0920-4105(01)00159-0.

Bedrikovetsky, P., Tran, T.L., Van den Broek, W.M.G.T., Marchesin, D., Rezende, E., Siqueira, A.G., Souza, A.L.S., and Shecaira, F.S. 2003. Damage Characterization of Deep-Bed Filtration From Pressure Measurements. *SPE Prod & Fac* **18** (2): 119–128. SPE-83673-PA. DOI: 10.2118/83673-PA.

Bedrikovetsky, P.G. 1993. *Mathematical Theory of Oil and Gas Recovery: With Applications to ex-USSR Oil and Gas Fields*, Vol. 4, ed. G. Rowan, trans. R. Loshak. Dordrecht, The Netherlands: Petroleum Engineering and Development Studies, Kluwer Academic Publishers.

Chauveteau, G., Nabzar, L., and Coste, J.-P. 1998. Physics and Modeling of Permeability Damage Induced by Particle Deposition. Paper SPE 39463 presented at the SPE Formation Damage Control Conference, Lafayette, Louisiana, USA, 18–19 February. DOI: 10.2118/39463-MS.

Elimelech, M., Jia, X., Gregory, J., and Williams, R.A. 1995. *Particle Deposition and Aggregation: Measurement, Modelling and Simulation*, hardcover edition. Woburn, Massachusetts: Colloid and Surface Engineering Series, Butterworth-Heinemann.

Eylander, J.G.R. 1988. Suspended Solids Specifications for Water Injection From Coreflood Tests. *SPE Res Eng* **3** (4): 1287–11294. SPE-16256-PA. DOI: 10.2118/16256-PA.

Herzig, J.P., Leclerc, D.M., and Goff, P. Le. 1970. Flow of Suspensions through Porous Media—Application to Deep Filtration. *Ind. Eng. Chem.* **62** (5): 8–35. DOI: 10.1021/ie50725a003.

Imdakh, A.O. and Sahimi, M. 1991. Computer simulation of particle transport processes in flow through porous media. *Chemical Engineering Science* **46** (8): 1977–1993. DOI: 10.1016/0009-2509(91)80158-U.

Iwasaki, T. 1937. Some notes on sand filtration. *J. of the American Water Works Association* **29**:1591–1602.

Khilar, K.C. and Fogler, H.S. 1998. *Migration of Fines in Porous Media*. Dordrecht, The Netherlands: Theory and Applications of Transport in Porous Media, Kluwer Academic Publishers.

Kuhnen, F., Barmettler, K., Bhattacharjee, S., Elimelech, M., and Kretzschmar, R. 2000. Transport of Iron Oxide Colloids in Packed Quartz Sand Media: Monolayer and Multilayer Deposition. *Journal of Colloid and Interface Science* **231** (1): 32–41. DOI: 10.1006/jcis.2000.7097.

Landau, L.D. and Lifshitz, E.M. 1980. *Statistical Physics*, Part 1, third edition, trans. J.B. Sykes and M.J. Kearsley, Vol. 5. Oxford, UK: Course in Theoretical Physics, Butterworth-Heinemann.

Moré, J.J., Garbow, B.S., and Hillstom, K.E. 1980. User guide for MINPACK-1. Report No. ANL-80-74, Argonne National Labs, Argonne, Illinois.

Nabzar, L., Coste, J.P., and Chauveteau, G. 1997. Water Quality and Well Injectivity. Paper 044 presented at the 9th European Symposium on Improved Oil Recovery, The Hague, 20–22 October.

Pang, S. and Sharma, M.M. 1997. A Model for Predicting Injectivity Decline in Water-Injection Wells. *SPE Form Eval* **12** (3): 194–201. SPE-28489-PA. DOI: 10.2118/28489-PA.

Payatakes, A.C., Tien, C., and Turian, R.M. 1973. A new model for granular porous media: Part I. Model formulation. *AIChE Journal* **19** (1): 58–76. DOI: 10.1002/aic.690190110.

Payatakes, A.S., Rajagopalan, R., and Tien, C. 1974. Application of Porous Medium Models to the Study of Deep Bed Filtration. *The Canadian Journal of Chemical Engineering* **52**: 727.

Rege, S.D. and Fogler, H.S. 1987. Network model for straining dominated particle entrapment in porous media. *Chemical Engineering Science* **42** (7): 1553–1564. DOI: 10.1016/0009-2509(87)80160-4.

Rege, S.D. and Fogler, H.S. 1988. A network model for deep bed filtration of solid particles and emulsion drops. *AIChE Journal* **34** (11): 1761–1772. DOI: 10.1002/aic.690341102.

Roque, C., Chauveteau, G., Renard, M., Thibault, G., Bouteca, M., and Rochon, J. 1995. Mechanisms of Formation Damage by Retention of Particles Suspended in Injection Water. Paper SPE 30110 presented at the SPE European Formation Damage Conference, The Hague, 15–16 May. DOI: 10.2118/30110-MS.

Sahimi, M. and Imdakh, A.O. 1991. Hydrodynamics of particulate motion in porous media. *Phys. Rev. Lett.* **66** (9): 1169–1172. DOI: 10.1103/PhysRevLett.66.1169.

Schechter, R.S. 1992. *Oil Well Stimulation*. Upper Saddle River, New Jersey: Prentice-Hall.

Shapiro A.A., Bedrikovetsky, P.G., Santos, A., and Medvedev, O.O. 2007. A stochastic model for filtration of particulate suspensions with incomplete pore plugging. *Transport in Porous Media* **67** (1): 135–164. DOI: 10.1007/s11242-006-0029-5.

Sharma, M.M. and Yortsos, Y.C. 1987. Transport of particulate suspensions in porous media: Model formulation. *AIChE Journal* **33** (10): 1636–1643. DOI: 10.1002/aic.690331007.

Sharma, M.M., Pang, S., Wennberg, K.E., and Morgenthaler, L.N. 2000. Injectivity Decline in Water-Injection Wells: An Offshore Gulf of Mexico Case Study. *SPE Prod & Fac* **15** (1): 6–13. SPE-60901-PA. DOI: 10.2118/60901-PA.

Siqueira, A.G., Bonet, E., and Shecaira, F.S. 2003. Network modelling for transport of water with particles in porous media. Paper SPE 18257 presented at the SPE Latin American and Caribbean Petroleum Engineering Conference, Port-of-Spain, Trinidad, West Indies, 27–30 April.

Soo, H., Williams, M.C., and Radke, C.J. 1986. A filtration model for the flow of dilute stable emulsions in porous media—II. Parameter evaluation and estimation. *Chemical Engineering Science* **41** (2): 273–281. DOI: 10.1016/0009-2509(86)87008-7.

van Oort, E., van Velzen, J.F.G., and Leerlooijer, K. 1993. Impairment by Suspended Solids Invasion: Testing and Prediction. *SPE Prod & Fac* **8** (3): 178–184; *Trans.*, AIME, **295**. SPE-23822-PA. DOI: 10.2118/23822-PA.

Veerapen, J.P., Nicot, B., and Chauveteau, G.A. 2001. In-Depth Permeability Damage by Particle Deposition at High Flow Rates. Paper SPE 68962 presented at the SPE European Formation Damage Conference, The Hague, 21–22 May. DOI: 10.2118/68962-MS.

Wennberg K.E. and Sharma M.M. 1997. Determination of the Filtration Coefficient and the Transition Time for Water Injection. Paper SPE 38181 presented at the SPE European Formation Damage Conference, The Hague, 2–3 June. DOI: 10.2118/38181-MS.

Appendix A—Analysis of the Solution Structure for the Multiple Capture System

Conditions of the particle mass conservation on the shock follow from Eqs. 6 and 7:

$$[C + S_1 + \dots + S_n] \frac{dx_f}{dt} = [C] \dots \dots \dots (A-1)$$

and

$$[S_i] \frac{dx_f}{dt} = 0, i = 1, 2 \dots n, \dots \dots \dots (A-2)$$

where $[C]$ and $[S_i]$ denote the jump in C and S_i , respectively, across the shock. From Eq. A-2 follows that retained concentrations are continuous functions, $[S_i] = 0$. Accounting for continuity of S_i in Eq. A-1, we obtain

$$[C] \frac{dx_f}{dt} = [C] \dots \dots \dots (A-3)$$

so, if the suspended concentration suffers a discontinuity, the shock speed is unity.

The characteristic form of Eq. 6 is

$$\frac{\partial C}{\partial T} + \frac{\partial C}{\partial X} = -(\Lambda_1(S_1, \dots, S_n) + \dots + \Lambda_n(S_1, \dots, S_n))C. \dots (A-4)$$

From the characteristic form of the system (Eqs. 6 and 7) and accounting for initial conditions (Eq. 11), it follows that all concentrations are zero ahead of the concentration front.

$$X > T : C(X, T) = S_i(X, T) = 0 \dots \dots \dots (A-5)$$

Appendix B—Reduction Procedure for the System of Multicapture Mechanism Equations

Eq. 10 is already in the characteristic form, in which the velocity of the characteristics is zero. Therefore, the retained concentrations fulfill a system of ordinary differential equations for $0 < X < 1$ and for $T > X > 0$.

$$\frac{1}{\Lambda_1(S_1, \dots, S_n)} \frac{dS_1}{dT} = \dots = \frac{1}{\Lambda_n(S_1, \dots, S_n)} \frac{dS_n}{dT} = C. \dots \dots (B-1)$$

From Eq. B-1 follows a system of n ordinary differential equations.

$$\frac{dS_i}{dS} = \frac{\Lambda_i(S_1, \dots, S_n)}{\sum_{i=1}^n \Lambda_i(S_1, \dots, S_n)}, i = 2, 3 \dots n, \dots \dots \dots (B-2)$$

where the total retained concentration is

$$S = \sum_{i=1}^n S_i \dots \dots \dots (B-3)$$

The retained concentrations are continuous functions (see Appendix A). Therefore, they equal zero along the concentration front $X = T$. This provides the initial condition for the system of ordinary differential equations (Eq. B-2).

$$S = 0 : S_i = 0 \text{ on } X = T \dots \dots \dots (B-4)$$

Let us denote the solution of the Cauchy problem (Eqs. B-2 and 4) as

$$S_i = f_i(S) \dots \dots \dots (B-5)$$

Now, we show that the system of deep-bed filtration of suspension with n dependent particle capture mechanisms is equivalent to that with the single mechanism of the particle capture by the rock. The sum of n equations (Eq. 10) gives the total capture rate

$$\frac{\partial S}{\partial T} = \left(\sum_{i=1}^n \Lambda_i(S_1, \dots, S_n) \right) C, \dots \dots \dots (B-6)$$

with the total filtration coefficient Λ

$$\Lambda(S_1, \dots, S_n) = \sum_{i=1}^n \Lambda_i(S_1, \dots, S_n). \dots \dots \dots (B-7)$$

Substitution of Eq. B-5 into Eq. B-7 results in the expression of the total filtration coefficient as a function of the total retained concentration.

$$\Lambda(S) = \sum_{i=1}^n \Lambda_i(S_1(f_i(S)), \dots, S_n(f_n(S))). \dots \dots \dots (B-8)$$

Finally, the system Eqs. 9 and 10 becomes

$$\begin{aligned} \frac{\partial}{\partial T}(C+S) + \frac{\partial C}{\partial X} &= 0 \\ \frac{\partial S}{\partial T} &= \Lambda(S)C \dots \dots \dots (B-9) \end{aligned}$$

Similar aggregation procedure can be applied for transport in porous media with multiple nonequilibrium adsorptions or with simultaneous irreversible chemical reactions (Bedrikovetsky 1993).

Appendix C—Examples for Aggregation of Several Capture Processes

Let us discuss first the example where the first filtration coefficient is a linear function of retained concentration and the second filtration coefficient is constant.

$$\lambda_1 = \lambda_0(h_0 - \sigma_1), \lambda_2 = \text{const.} \dots \dots \dots (C-1)$$

In this case, rewriting Eq. B-2 in terms of σ_1, σ_2 allows for the first integral

$$\frac{\sigma_2}{\lambda_2} = \int_0^{\sigma_1} \frac{d\sigma}{\lambda_0(h_0 - \sigma)} = \frac{\ln(h_0 - \sigma_1)}{\lambda_0} \dots \dots \dots (C-2)$$

This gives total retained concentration $\sigma = \sigma_1 + \sigma_2$.

$$\sigma(\sigma_1) = \ln(h_0 - \sigma_1)^{\frac{\lambda_2}{\lambda_0}} + \sigma_1 \dots \dots \dots (C-3)$$

and, thus, expresses σ_1 in terms of σ through the inverse of Eq. C-3. The final expression for the overall filtration coefficient is

$$\lambda(\sigma) = \lambda_0(h_0 - \sigma_1(\sigma)) + \lambda_2 \dots \dots \dots (C-4)$$

As a second example, let the first filtration coefficient be quadratic and the second filtration coefficient be constant.

$$\lambda_1 = a(S_1 + b)^2, \lambda_2 = d \dots \dots \dots (C-5)$$

In this case, Eq. B-2 allows for the first integral.

$$\frac{S_2}{d} = \int_0^{S_1} \frac{ds}{a(s+b)^2} = \frac{S_1}{ab(S_1+b)} \dots \dots \dots (C-6)$$

The total deposited concentration can be expressed via the first retained concentration.

$$S = S_1 + S_2 = S_1 + \frac{S_1 d}{ab(S_1 + b)} \dots \dots \dots (C-7)$$

The inverse function to Eq. C-7 allows expressing the first retained concentration via the total deposited concentration.

$$S_1 = \frac{1}{2} \left(S - \frac{d}{ab} - b \pm \sqrt{\left(S - \frac{d}{ab} - b \right)^2 + 4Sb} \right) \dots \dots \dots (C-8)$$

Substitution of Eq. C-8 into Eq. C-5 results in the following form for the overall filtration coefficient

$$\lambda(S) = d + \frac{a}{4} \left(S - \frac{d}{ab} + b \pm \sqrt{\left(S - \frac{d}{ab} - b \right)^2 + 4Sb} \right)^2 \dots \dots \dots (C-9)$$

Appendix D—Example of Deep-Bed Filtration of Hematite Particles With Monolayer and Poly-layer Adsorption

The system consists of mass-balance equations for suspended and adsorbed particles, a kinetic equation for overall retention rate, and a blocking kinetic equation for monolayer adsorption (Kuhnen et al. 2000).

$$\frac{\partial}{\partial t} [c + fc_s] + v_p \frac{\partial c}{\partial x} = 0 \dots \dots \dots (D-1)$$

$$\frac{\partial c_s}{\partial t} = [k_{pc}B(\theta) + k_{pp}\theta]c \dots\dots\dots (D-2)$$

$$\frac{\partial \theta}{\partial t} = k_{pc}B(\theta)\pi a_p^2 c \dots\dots\dots (D-3)$$

Here, v_p is the average interstitial velocity of colloidal particles, f is the bare matrix surface area available for colloid deposition per unit pore volume, c_s is surface concentration of deposited particles, k_{pc} is the deposition rate of colloidal particles to bare matrix surfaces, k_{pp} is the deposition rate of colloidal particles to previously deposited particles attached to matrix surfaces, a_p is the grain diameter, θ is the fraction of the bare surface covered with colloidal particles, and $B(\theta)$ is a so-called dynamic blocking function.

Translation of the surface retention concentration c_s into volumetric retention concentration σ and introduction of dimensionless parameters

$$\sigma = \phi f c_s, \quad U = \phi v_p, \quad \varsigma = \frac{k_{pc} L f}{v_p},$$

$$\varepsilon = \frac{k_{pp}}{k_{pc}}, \quad \text{and} \quad \gamma = k_{pc} \frac{\phi L \pi a_p^2 c^0}{U} \dots\dots\dots (D-4)$$

transforms Eqs. D-1, D-2, and D-3) into the dimensionless form (Eqs. 6, 14, and 15).

The number of independent parameters can be reduced to two, β and ε , as follows (Kuhnen et al. 2000). The deposition rates k_{pc} and k_{pp} can be interpreted as the product of the fast deposition rate under favorable conditions k^f (in the absence of electrostatic repulsive or attractive forces) and a collision efficiency for particle/matrix and particle/particle interactions, respectively. Thus $k_{pc} = k^f \alpha_{pc}$ and $k_{pp} = k^f \alpha_{pp}$. The initial deposition rate under favorable conditions, k^f , can be calculated from filtration theory (Elimelech et al. 1995). The collision efficiency for particle/particle interactions α_{pp} can be measured in laboratory (Kuhnen et al. 2000). Therefore, both ς and γ can be expressed in terms of ε .

Initial and boundary conditions are given by Eq. 3. The condition of initial absence of particles on the grain surface

$$T = 0: \theta = 0 \dots\dots\dots (D-5)$$

must be added to the boundary conditions to describe suspension injection into a particle-free rock.

The aggregation procedure is similar to that for Eqs. 17 through 20. Let us choose the total retention concentration S as an independent variable in the system of ordinary differential equations along characteristics with zero speed. This reduces the system to one ordinary differential equation.

$$\frac{d\theta}{dS} = \frac{\gamma B(\theta)}{\varsigma [B(\theta) + \varepsilon \theta]} \dots\dots\dots (D-6)$$

A new constant ξ is defined by

$$\xi = \frac{\varsigma}{\gamma} \dots\dots\dots (D-7)$$

The first integral of Eq. D-6 is

$$S = \xi \int_0^\theta \left(1 + \frac{\varepsilon y}{B(y)} \right) dy = \xi \theta + \xi \varepsilon \int_0^\theta \frac{y dy}{B(y)} \dots\dots\dots (D-8)$$

Eq. D-8 can be calculated explicitly for the case of Langmuir blocking sorption (Eq. 16).

$$S = -\xi \left[\theta \left(\frac{\varepsilon}{\beta} - 1 \right) + \frac{\varepsilon}{\beta^2} \ln(1 - \beta \theta) \right] \dots\dots\dots (D-9)$$

Finally, the overall filtration coefficient is

$$\Lambda(S) = \varsigma [1 + (\varepsilon - \beta)\theta(S)], \dots\dots\dots (D-10)$$

where $\theta(S)$ is the inverse function to Eq. D-9. This inverse function can be calculated explicitly in case $\varepsilon = 0$, where the particle/particle interaction vanishes at low brine ionic strength. In this case,

$$S = \xi \theta \dots\dots\dots (D-11)$$

and the total filtration coefficient is

$$\Lambda(S) = \varsigma \left[1 - \beta \frac{S}{\xi} \right] \dots\dots\dots (D-12)$$

R.G. Guedes was a BS student of the Department of Petroleum Exploration and Production at North Fluminense State University while working on this paper. He graduated with distinction and currently is a drilling engineer with Weatherford in Brazil. **Firas Al-Abduwani** holds a BS degree in mechanical engineering from Imperial College, an MEng degree in petroleum engineering from Heriot-Watt University, and a PhD degree from Delft University of Technology in produced water management. His studies were sponsored by a scholarship from Petroleum Development of Oman. Al-Abduwani is currently managing director of a company in Oman working in telecommunications and data networks. **Pavel Bedrikovetsky** is the author of two books on reservoir engineering and 140 technical papers. His research covers formation damage, enhanced oil recovery and nonlinear mathematical physics. He holds an MS degree in applied mathematics, a PhD degree in fluid mechanics and a DSc degree in reservoir engineering from Gubkin Russian State University of Oil and Gas. Since 1994, he has been senior staff consultant at Petrobras. He served as section chairman, short course instructor, key speaker, and Program Committee member at several SPE conferences and Applied Technology Workshop. He was a 2008-09 SPE distinguished lecturer. Since 2008, Bedrikovetsky has been professor, chair in petroleum engineering at the Australian School of Petroleum, University of Adelaide. **Peter Currie** recently retired from the professorship in oil and gas production at Delft University of Technology. He holds a BS degree in mathematics from the University of Manchester and a PhD degree in theoretical mechanics from the University of East Anglia. He worked for Shell for many years in the area of production technology, both in research and operations. He joined Delft University of Technology in 1997. He has been chairman of the Netherlands SPE Section and has served on the SPE International Board as Director for Europe and Africa.